BRIEF COMMUNICATIONS

The purpose of this Brief Communications section is to present important research results of more limited scope than regular articles appearing in Physics of Fluids A. Submission of material of a peripheral or cursory nature is strongly discouraged. Brief Communications cannot exceed three printed pages in length, including space allowed for title, figures, tables, references, and an abstract limited to about 100 words.

Particle orbits from the Lagrangian and the Eulerian Korteweg–de Vries equations

A. Provenzale and A. R. Osborne
Istituto di Cosmogeofisica del CNR, Corso Fiume 4, Torino 10133, Italy

G. Boffetta and M. Serio
Istituto di Fisica Generale dell'Universitá, C. M.d'Azeglio 46, Torino 10125, Italy

(Received 13 September 1989; accepted 10 January 1990)

The particle orbits obtained by integrating the velocity field of the Eulerian Korteweg–deVries (KdV) equation and the trajectories given by the Lagrangian KdV equation are contrasted. It is shown that the two classes of orbits, while apparently equivalent, may be quite different. In particular, a spurious wave drift is generated by integrating the Eulerian velocities. It is shown that these differences are due to a mixing of perturbation orders inherent in the integration of the Eulerian velocity field. It is believed that these results may have some implications on the calculation of particle orbits in Eulerian flow models obtained by a perturbation expansion of the primitive equations.

The study of fluid flows in Lagrangian coordinates focuses on the motion of individual fluid particles. In a previous paper[1] we derived the Korteweg–deVries (hereafter known as KdV) equation in Lagrangian coordinates, and in a subsequent work[2] the results were extended to the nonlinear Schrödinger equation. In Refs. 1 and 2 we used the classic approach for the Lagrangian description of fluid flows, where the dynamical (dependent) variables are the positions of all the fluid particles and the independent variables are the time and the positions of the particles at rest.[3] This approach results in a set of partial differential equations (field equations) that must be complemented by appropriate boundary and initial conditions.

A different approach to the study of fluid flows in Lagrangian coordinates is, however, possible. In this context the particle orbits are obtained by appropriately integrating the velocity field provided by the Eulerian equations of motion [see system (4) below]. This approach has been extensively used, e.g., in Refs. 4–12, in the study of chaotic advection. In this Brief Communication we show that the orbits obtained using such an approach may, in certain cases, spuriously differ from the particle trajectories provided by a direct Lagrangian formulation. This occurs when the Eulerian flow model is obtained by a perturbation expansion of the primitive equations and it is due to a mixing of perturbation orders in system (4) below. The case of the KdV equation is used as an explicit example of this type of problem.

First we recall the properties of the Lagrangian KdV equation (L–KdV). This is obtained from the surface wave problem in Lagrangian coordinates by a regular perturbation expansion in powers of a nonlinearity parameter $\epsilon = \eta_0/h$ (where η_0 is a typical wave amplitude and h is the water depth) and of a dispersion parameter $\delta^2 = (h/L)^2$ (where L is a typical wavelength). The KdV model is found at $O(\epsilon)$ and $O(\delta^2)$ with the further requirement that ϵ and δ^2 are of the same order of magnitude. At this order the evolution equations for the particle positions are[1]

$$X_t + c_0 X_a - (\alpha h/2) X_a^2 + \beta X_{aaa} + C = 0, \tag{1a}$$

$$Y_t + c_0 Y_a + (\alpha h/b) Y Y_a + \beta Y_{aaa} = 0. \tag{1b}$$

The dependent variables are $X = x(a,t) - a$ and $Y = y(a,b,t) - b$, where (x,y) is the position of a fluid particle at time t and (a,b) is the position of the particle at rest. Subscripts a and t indicate partial derivatives; $c_0 = (gh)^{1/2}$, $\alpha = 3c_0/2h$, and $\beta = c_0 h^2/6$ are constant, g is the acceleration of gravity, and h is the water depth. Note that the above constants have the same definition as in the Eulerian approach.[13] The constant C in Eq. (1a) is given by

$$C = \frac{\alpha}{2hL} \int_a^{a+L} \eta^2(a,t)\,da,$$

in the infinite-line limit $L \to \infty$ and $C \to 0$. The two evolution equations [(1a) and (1b)] may be summarized by a single KdV equation,

$$\eta_t + c_0 \eta_a + \alpha \eta \eta_a + \beta \eta_{aaa} = 0, \tag{2}$$

with the definitions

$$\eta(a,t) = -h \frac{\partial X(a,t)}{\partial a}, \tag{3a}$$

$$Y(a,b,t) = (b/h)\eta(a,t). \tag{3b}$$

A different approach to the study of fluid particle motions is based on considering the dynamics of a single-fluid particle, which is subjected to a given Eulerian velocity field:

$$\frac{d\mathbf{x}}{dt} = \mathbf{u}(\mathbf{x},t), \tag{4}$$

where $\mathbf{x}(t) = (x(t),y(t))$ is the position of the fluid particle and $\mathbf{u}(\mathbf{x},t) = (u(\mathbf{x},t),v(\mathbf{x},t))$ is the Eulerian velocity at point

 0899-8213/90/050866-04$02.00

x and at time t. Note that in (4) we have considered a two-dimensional fluid.

While apparently equivalent, the two approaches depicted above may in some cases provide different particle orbits. To elucidate this problem we consider some examples of the use of system (4) with u and v given by a particular solution of the Eulerian KdV (E–KdV) equation, together with the corresponding orbits predicted by the L–KdV equation. The E–KdV equation is given by[13]

$$\eta_t + c_0\eta_x + \alpha\eta\eta_x + \beta\eta_{xxx} = 0, \tag{5}$$

where $\eta(x,t)$ is the surface elevation and the constants c_0, α, and β have been defined above. At the KdV order of approximation the relationship between the velocity field and the surface elevation is given by

$$u = c_0(\eta/h), \tag{6a}$$

$$v = -c_0(y/h)\eta_x, \tag{6b}$$

i.e., the velocity field is entirely determined by the knowledge of the surface elevation. Thus the form of $\eta(x,t)$ defines the Eulerian flow structure entirely.

First we consider the case of a single soliton. This solution of the KdV equation is written in Eulerian coordinates as

$$\eta(x,t) = \eta_0 \operatorname{sech}^2[K(x - x_0) - \Omega t], \tag{7}$$

where the amplitude η_0, the wavenumber K, and the frequency Ω are related by

$$\eta_0 = 2(K^2/\lambda),$$

$$\Omega = c_0K + 4\beta K^3,$$

and $\lambda = \alpha/6\beta$. The corresponding single-soliton solution of the L–KdV equation is obtained from (7) by the substitution $x \to a$. In Fig. 1 we report the orbit of a fluid particle during the passage of a soliton, known to be a parabola.[1] The solid curve is obtained from the single-soliton solution of the L–KdV equation while the dashed curve is obtained from integration of system (4) with u given by formula (7) and Eqs. (6a) and (6b). As we can see, the two orbits are different.

The second type of example is provided by the (periodic) cnoidal wave solution of the KdV equation. The Eulerian form of the cnoidal wave is

$$\eta(x,t) = 2\eta_c cn^2\{[K(m)/\pi][k(x - x_0) - \omega t];m\} - \eta_m, \tag{8}$$

where the amplitude η_c, the wavenumber $k = 2\pi/L$, and the modulus m of the cnoidal wave are related by

$$m K^2(m) = (3\pi^2/2k^2h^3)\eta_c, \tag{9}$$

and $K(m)$ is the complete elliptic integral of the first kind. The cnoidal wave (8) has zero mean, the constant η_m is given by

$$\eta_m = 2\eta_c + 4k^2h^3K(m)[E(m) - K(m)]/3\pi^2, \tag{10}$$

and the frequency ω is given by

$$\omega = c_0k - \beta k^3 + c_0k\{-\eta_c/h + (k^2h^2/6\pi^2) \times [\pi^2 - 4K(m)(3E(m) - 2K(m))]\}, \tag{11}$$

where $E(m)$ is the complete elliptical integral of the second kind. The cnoidal wave solution of the L–KdV equation may be obtained from formula (8) by the substitution $x \to a$. Again, we may compute a particle orbit by deriving the Eulerian velocity field for the cnoidal wave (8) through Eqs. (6a) and (6b) and by subsequently using it in system (4). In Figs. 2(a) and 2(b) we report the orbits obtained in this way (dashed line) together with the orbits obtained as exact cnoidal wave solutions of the L–KdV equation (solid line) for two different values of the modulus of the cnoidal wave. The orbits drawn in Figs. 2(a) and 2(b) refer to particles that have the same vertical rest position, both in the L–KdV and in the E–KdV approach. The orbits obtained with the

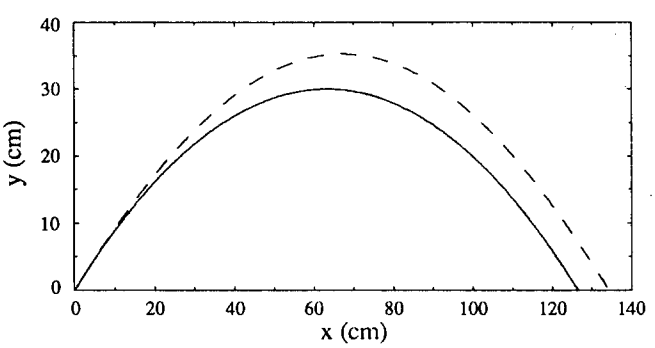

FIG. 1. Particle orbits for the single-soliton solution of the KdV equation. The solid line indicates the solution of the L–KdV equation and the dashed line indicates the solution given by inserting the Eulerian KdV velocity field into system (4) in the text. Parameters are $h = 100$ cm and $\eta_0 = 30$ cm. The reference position of the particle is $a = 0$, $b = h$, i.e., the particle is on the surface.

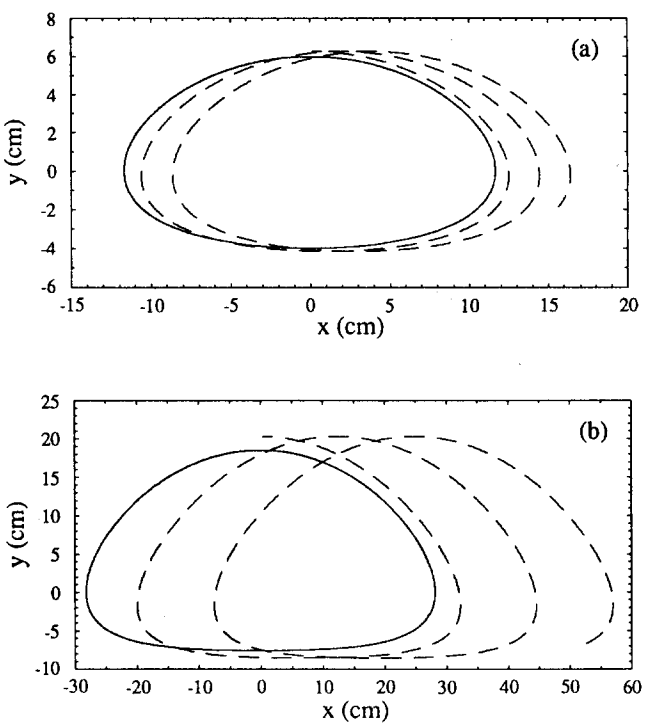

FIG. 2. Particle orbits for the cnoidal wave solution of the KdV equation. The solid lines indicate the solution of the L–KdV equation and the dashed lines indicate the solution given by inserting the Eulerian KdV velocity field into system (4) in the text. For panel (a) the parameters are $h = 100$ cm, $L = 1500$ cm, $2\eta_c = 10$ cm, and the modulus of the cnoidal wave is 0.81; for panel (b) the parameters are $h = 100$ cm, $L = 1500$ cm, $2\eta_c = 26$ cm, and the modulus of the cnoidal wave is 0.98. The reference positions of the particles are $a = 0$, $b = h$, i.e., the particles are on the surface.

direct Lagrangian approach and with the use of system (4) are different. In particular, the orbits obtained by integrating the system (4) display a spurious particle drift that is well known to be absent at the order of approximation of the KdV equation.[1,14] Physically, the lack of the Stokes drift in the KdV model may be understood by recalling that this drift is generated by the joint effect of a noninfinitesimal wave amplitude and of a vertical dependence of the horizontal velocity, a fact that induces nonclosed particle orbits. By contrast, the horizontal velocity is independent of the vertical coordinate in the KdV approximation; consequently, no Stokes drift is generated. Also note that the orbits obtained from system (4) plus expressions (6a) and (6b) have slightly larger amplitudes than the orbits given by the L–KdV equation.

The above examples show that one is faced with the problem of two apparently equivalent descriptions that provide different results. A natural first question to ask is whether the solutions obtained by the Eulerian procedure and by the Lagrangian procedure correspond to the same flow. This is equivalent to asking whether the same functional form of the Eulerian free surface $\eta_E(x,t)$ and of the Lagrangian free surface $\eta_L(a,t)$ generates the same flow, i.e., whether $\eta_E(x=a,t)=\eta_L(a,t)$ at the KdV order of approximation. To answer this question we note first that, by definition, the free surface has the property $\eta_E[x(a,t),t]=\eta_L(a,t)$. From this we may write $\eta_E(x,t)=\eta_E(a+X,t)$, where a is the rest position of a particle and $X=x-a$ is the horizontal displacement of the particle from its rest position. We may Taylor expand the above expression and obtain $\eta_E(x,t)=\eta_E(x=a,t)+X(\partial\eta_E/\partial x)_{x=a}+\cdots$. Next we note that the surface η_E/h is order ϵ, and that each space derivative brings out a factor $\epsilon^{1/2}$, see, for example, Segur.[13] From system (4) plus expression (6a) we obtain that dx/dt is of order ϵ, and since each time derivative also brings out a factor $\epsilon^{1/2}$, we have that $X=x-a$ is order $\epsilon^{1/2}$. Thus the second term in the Taylor expansion of $\eta(a+X,t)$ is order ϵ^2, beyond the KdV order of approximation. As a consequence, at the KdV order of approximation we have that $\eta_L(a,t)=\eta_E[x(a,t),t]=\eta_E(x=a,t)$, and the same functional form of the Eulerian free surface and of the Lagrangian free surface corresponds to the same flow structure.

The kind of arguments introduced above completely explain the observed differences between the E–KdV and the L–KdV trajectories. As mentioned above, the discrepancy between the two classes of orbits is in fact due to a mixing of perturbation orders generated by the *naif* use of system (4). Combining system (4) and expressions (6a) and (6b) we obtain for the particle orbits in the KdV model[13]

$$\frac{dx}{dt}=c_0\frac{\eta(x(a,t),t)}{h}\{1+O(\epsilon)\} \tag{12a}$$

$$\frac{dy}{dt}=-c_0\gamma\frac{\eta_x(x(a,t),t)}{h}\{1+O(\epsilon)\}, \tag{12b}$$

where $\eta/h\approx O(\epsilon)$ and $\eta_x/h\approx O(\epsilon\delta)\approx O(\epsilon^{3/2})$. However, the rhs terms of both Eqs. (12a) and (12b) also contain terms that generate effects of order higher than ϵ or δ^2 and that must be discarded to be consistent with the KdV approximation. Considering for simplicity $\delta^2=\epsilon$ (consistently with the assumptions made in deriving the KdV) in Eqs. (12a) and (12b) we have, in fact, that

$$\eta_x=-(1/c_0)\eta_t\{1+O(\epsilon)\}. \tag{13}$$

In addition, by Taylor expanding $\eta(x(a,t),t)$ around the spatial position a we have that $\eta(x(a,t),t)/h=(\eta(a,t)/h)\times\{1+O(\epsilon)\}$ and, using Eq. (13), that $c_0\eta_x(x(a,t),t)/h=(\eta_t(a,t)/h)\{1+O(\epsilon)\}$. Thus, finally,

$$\frac{dx}{dt}=c_0\frac{\eta(a,t)}{h}\{1+O(\epsilon)\}, \tag{14a}$$

$$\frac{dy}{dt}=b\frac{\eta_t(a,t)}{h}\{1+O(\epsilon)\}. \tag{14b}$$

Systems (14a) and (14b) are now at the same order of approximation of the KdV equation. Using the surface elevation $\eta(a,t)$ in the point a and at time t given by the E–KdV equation we immediately obtain the expressions (3a) and (3b) for $x(a,t)$ and for $y(a,b,t)$. Considering for simplicity the infinite-line problem, at the order of the KdV equation, we have, in fact, that

$$y(a,b,t)=\frac{b}{h}\int_{-\infty}^{t}\eta_{t'}\,dt'\{1+O(\epsilon)\},$$

i.e.,

$$y(a,b,t)-b=(b/h)\eta(a,t)\{1+O(\epsilon)\},$$

which is the same expression given in Eq. (3b). By differentiating expression (14a) with respect to a, we obtain for the horizontal motions

$$\frac{d}{dt}x_a(a,b,t)=\frac{c_0}{h}\eta_a+o(\epsilon,\delta^2)=-\frac{1}{h}\eta_t\{1+O(\epsilon)\},$$

and by integrating this expression with respect to time from $-\infty$ to t we have

$$-\frac{\partial}{\partial a}[x(a,t)-a]=\frac{\eta(a,t)}{h}\{1+O(\epsilon)\},$$

as in formula (3a). In this way, retaining the correct order of approximation, the use of system (4) with the velocity field provided by the E–KdV equation provides the same particle orbits obtained by directly integrating the L–KdV equation. The discrepancies observed in the examples discussed above were thus entirely due to the use of Eqs. (12a) and (12b) without the elimination of the higher-order terms. These terms are totally spurious since they are not balanced by any quantities at the same order of approximation in the expression for the Eulerian velocity field.

We believe that the results discussed here may have some general implications since they indicate that system (4) must be used with caution when considering (exact) solutions of Eulerian models that are obtained through perturbation expansions of the primitive equations. When system (4) is used with u and v, given by an exact solution of the Euler or Navier–Stokes equations (such as in the case of the Arnold–Beltrami–Childress flow[7]), or when it is used in connection with particular models of the Eulerian velocity field (such as in the case of two intermittent vortex singularities[4]) the problems discussed in this Brief Communication are not relevant. On the other hand, the use of system (4) with a velocity field given by an exact solution of some ap-

proximate form of the Euler equations may generate particle orbits that are not consistent with the order of approximation of the Eulerian model. In this case, it would be misleading to claim that the observed trajectories are the correct particle orbits at the order of approximation of the Eulerian model employed. In all these cases, a careful evaluation of the perturbation orders is required in order to resolve the issues raised herein. Also, for such problems a direct derivation of the equations of motion in Lagrangian coordinates (as done for the case of the KdV equation[1]) may be desirable.

[1]A. R. Osborne, A. D. Kirwan, Jr., A. Provenzale, and L. Bergamasco, Phys. Fluids **29**, 656 (1986).
[2]A. R. Osborne and G. Boffetta, Phys. Fluids A **1**, 1200 (1989).
[3]H. Lamb, *Hydrodynamics* (Cambridge U.P., Cambridge, 1932).
[4]H. Aref, J. Fluid Mech. **143**, 1 (1984).
[5]H. Aref and S. Balachandar, Phys. Fluids **29**, 3515 (1986).
[6]H. Aref, S. W. Jones, and G. Tryggvason, Complex Syst. **1**, 545 (1987).
[7]T. Dombre, U. Frisch, J. M. Greene, M. Henon, A. Mehr, and A. M. Soward, J. Fluid Mech. **167**, 353 (1986).
[8]J. Chaiken, C. K. Chu, M. Tabor, and Q. M. Tan, Phys. Fluids **30**, 687 (1987).
[9]W. L. Chien, H. Rising, and J. M. Ottino, J. Fluid Mech. **170**, 355 (1986).
[10]D. V. Khakhar and J. M. Ottino, Phys. Fluids **29**, 3503 (1986).
[11]D. V. Khakhar, H. Rising, and J. M. Ottino, J. Fluid Mech. **172**, 419 (1986).
[12]M. Pettini, A. Vulpiani, J. H. Misguich, M. De Leener, J. Orban, and R. Balescu, Phys. Rev. A **38**, 344 (1988).
[13]M. J. Ablowitz and H. Segur, *Solitons and the Inverse Scattering Transform* (SIAM, Philadelphia, 1981).
[14]F. Ursell, Proc. Cambridge Philos. Soc. **49**, 685 (1953).

Free-stream turbulence: A limitation on fractal descriptions of open-flow systems

Steven P. Schneider
School of Aeronautical and Astronautical Engineering, Purdue University, West Lafayette, Indiana 47907

(Received 7 April 1989; accepted 28 December 1989)

Cylinder wake velocity measurements were made at Reynolds number 100 with varying levels of free-stream turbulence. The Grassberger–Procaccia (G–P) correlation function, which is often used for estimating fractal dimension, was computed for these data, and also for data obtained by adding random noise to the iterations of the Henon map. A comparison of the two plots shows that the free-stream turbulence acts as a highly random external noise source. Since free-stream turbulence determines the details of the smaller flow scales, no low-order dynamical system will be able to model all the scales in this open flow.

Fractal descriptions of turbulent and transitional flow have recently been a popular and sometimes controversial topic of research (see, e.g., Refs. 1–4). The low-Reynolds-number wake of a circular cylinder was chosen as a test case for the applicability of chaos concepts to open-flow systems because it is a classical open-flow oscillator. This wake has often been studied, perhaps most recently by Williamson.[5] For Reynolds numbers of roughly 50 to 180, the wake consists of alternately shed laminar vortices, which give rise to periodic velocity fluctuations at a fixed point in the wake. It is considered to be an open-flow system because the flow contains at least one open boundary across which fluid flows from some other region. In this case, the nominally uniform wind tunnel free stream crosses the upstream boundary to flow over the cylinder, and then crosses the downstream boundary into the wind tunnel diffuser.

When this work began, it was hoped that the free-stream turbulence would act only as the small error in the initial conditions of a low-order chaotic system such as the Henon map, so that the wake velocities would scale as a fractal all the way down to the viscous scales. However, it will be shown that free-stream turbulence acts instead as an *added* source of noise. This result provides a significant quantitative small-scale limitation to fractal descriptions of turbulent and transitional flow. Although it has been known for some time that any fractal scaling region must have a lower cutoff set by noise, the author believes that this Brief Communication provides the first clear evidence that free-stream turbulence can cause such a noise cutoff in an open flow. A quantitative relation between the turbulence level and the noise cutoff level is also provided.

Cylinder wake velocity measurements were made in an open-return wind tunnel at Reynolds number 100. The cylinder (diameter 0.0825 in.) was placed normal to the flow, and spanned the 20 in. width of the square test section. A hot wire was placed parallel to the cylinder in order to measure the streamwise component of velocity. The hot wire was located at the cylinder midspan, about ten diameters downstream of the cylinder, and about one diameter off the centerline, just out of the frequency-doubling region. The vortex-shedding frequency was 58 Hz. The single-sensor TSI hot wire was operated at constant temperature using anemometers similar to those used by Cimbala *et al.*[6] The data were digitized at 4 kHz using a computer system constructed locally.[7] Raw voltage data were converted to velocity using a King's law calibration, although the dimension results were

0899-8213/90/050869-04$02.00